JPET Fast Forward. Published on May 2, 2013 as DOI: 10.1124/jpet.113.203265

Basolateral Uptake of Nucleosides by Sertoli Cells is Mediated Primarily by Equilibrative Nucleoside Transporter 1 (ENT1).

David M. Klein, Kristen K. Evans, Rhiannon N. Hardwick, William H. Dantzler, Stephen H. Wright, Nathan J. Cherrington

University of Arizona, Department of Pharmacology and Toxicology, 1703 E Mabel St, Tucson, AZ, 85721, United States (D.M.K., R.N.H., N.J.C.)

University of Arizona, Department of Physiology, Tucson, AZ, 85721, United States (K.K.E., W.H.D., S.H.W.)

JPET Fast Forward. Published on May 2, 2013 as DOI: 10.1124/jpet.113.203265
This article has not been copyedited and formatted. The final version may differ from this version.

Running Title: ENT1 is Responsible for Nucleoside Uptake into Sertoli Cells

Corresponding author: Nathan J. Cherrington

1703 E Mabel

PO Box 210207

Tucson AZ 85721

PH: (520) 626-0219

Fax: (520) 626-2466

cherrington@pharmacy.arizona.edu

Text Pages: 30

Tables: 1

Figures: 10

References: 41

Words in Abstract: 239

Words in Introduction: 748

Words in Discussion: 1,323

Abbreviations: ENT, equilibrative nucleoside transporter; BTB, blood-testis barrier; NBMPR, nitrobenzylmercaptopurine riboside or 6-*S*-[(4-Nitrophenyl)methyl]-6-thioinosine; NRTI, nucleoside reverse transcriptase inhibitor; IHC, immunohistochemistry; MGT, male genital tract; AZT, zidovudine; ddI, didanosine; TDF, tenofovir disoproxil fumarate.

Recommended Section Assignment: Metabolism, transport and pharmacogenomics

Abstract

The blood-testis barrier (BTB) prevents the entry of many xenobiotic compounds into seminiferous tubules thereby protecting developing germ cells. Understanding drug transport across the BTB may improve drug delivery into the testis. Members of one class of drug, nucleoside reverse transcriptase inhibitors (NRTIs), do penetrate the BTB, presumably through interaction with physiological nucleoside transporters. By investigating the mechanism of nucleoside transport, it may be possible to design other drugs to bypass the BTB in a similar manner. We present a novel *ex vivo* technique to study transport at the BTB that employs isolated, intact seminiferous tubules. Using this system, we found that over 80% of total uptake by seminiferous tubules of the model nucleoside uridine could be inhibited by 100 nM nitrobenzylmercaptopurine riboside (NBMPR), a concentration that selectively inhibits equilibrative nucleoside transporter 1 (ENT1) activity. In primary cultured rat Sertoli cells, 100 nM NBMPR inhibited all transepithelial transport and basolateral uptake of uridine. Immunohistochemical (IHC) staining showed ENT1 to be located on the basolateral membrane of human and rat Sertoli cells, whereas ENT2 was located on the apical membrane of Sertoli cells. Transepithelial transport of uridine by rat Sertoli cells was partially inhibited by the NRTIs zidovudine, didanosine, and tenofovir disoproxil fumarate, consistent with an interaction between these drugs and ENT transporters. These data indicate that ENT1 is the primary route for basolateral nucleoside uptake into Sertoli cells and a possible mechanism for nucleosides and nucleoside-based drugs to undergo transepithelial transport.

Introduction

The anatomical portion of the blood-testis barrier (BTB) is composed of tight junctions formed between the Sertoli cells that line the seminiferous tubules inside the testis (Pelletier, 2011; Mital, et al, 2011; Li et al, 2012). This barrier prevents many exogenous agents from gaining entry into the lumen of the seminiferous tubules and contacting germ cells. It is also the responsibility of the Sertoli cells to provide nutrients such as nucleosides that allow for spermatogenesis (Kato et al, 2009; Mruk and Cheng, 2011). Although this barrier is beneficial for sperm cell development, it can be an obstacle for drugs that are required to bypass the BTB to achieve full therapeutic effect. Examples of such drugs include many antiretroviral medications used to treat infection of human immunodeficiency virus (HIV). By limiting the entry of many antiretrovirals into the male genital tract (MGT), the BTB may be contributing to the testes' serving as a sanctuary site for HIV (Byrn and Kiessling, 1998; Anderson et al, 2000; Olson, 2002; Dahl et al, 2010). Since the tight junctions of the BTB prevent paracellular diffusion of hydrophilic drugs, transcellular transport through the Sertoli cells is required for antiretrovirals to bypass the BTB.

One class of HIV antiretrovirals, nucleoside reverse transcriptase inhibitors (NRTIs), may be able to bypass the BTB (Augustine et al, 2005; Else et al, 2011; Pereira et al, 2002). Clinical data have shown seminal plasma concentrations of zidovudine (AZT) and didanosine (ddI) are up to 10 fold higher than blood plasma (Prins et al, 2007; Dumond et al., 2008). Understanding the transepithelial transport pathway NRTIs use to bypass the BTB could potentially be useful in designing other drugs to cross into the lumen of seminiferous tubules.

Since NRTIs are nucleoside analogs, these medications may use the same nucleoside transport pathway(s) used by endogenous nucleosides, such as uridine. Currently, Kato *et al* represent the field's understanding of the physiological pathway for nucleosides crossing the BTB (Kato et al 2005). They found that uridine uptake into primary Sertoli cells is dominated by two sodium

JPET Fast Forward. Published on May 2, 2013 as DOI: 10.1124/jpet.113.203265
This article has not been copyedited and formatted. The final version may differ from this version.

independent components which possess characteristics similar to equilibrative transporter 1 (ENT1) and equilibrative transporter 2 (ENT2). ENT proteins are bidirectional transporters that facilitate nucleosides transport according to concentration gradient (Ward et al, 2000; Baldwin et al, 2004). Function of ENT1 and ENT2 is commonly differentiated based on their relative sensitivity to NBMPR; ENT1 is very sensitive to NBMPR inhibition (K_i= 0.1 to 68.5 nM), ENT2 is unaffected by NBMPR at concentrations up to 1μM, but is blocked by 100 μM NBMPR (Griffiths et al, 1997; Takano et al, 2010; Yao et al, 2011; Abd-Elfattah et al, 2012; Nishimura et al, 2012). ENT1 and ENT2 have been shown to transport AZT and are speculated to transport other NRTI drugs as well (Ward et al, 2000; Pastor-Anglada et al, 2005). It has also been shown that basolateral entry of nucleosides into Sertoli cells is ENT dependent, although it has not been clear whether ENT1, ENT2, or both are involved (Kato et al, 2005). A minor sodium dependent component was also found to contribute to uridine uptake which was ascribed to be a concentrative nucleoside transporter (CNT). CNT proteins are unidirectional uptake transporters that typically localize to the apical membrane of epithelial cells and usually play a role in nucleoside salvaging (Kato et al, 2005; Lu et al, 2004; Errasti-Murugarren et al, 2012). NBMPR does not interact with CNT transporters allowing it to be a tool for distinguishing between ENT and CNT mediated transport (Ritzel et al, 2000; Kong et al, 2004; Fernandez-Calotti et al, 2011; Nishimura et al, 2012).

Despite the work done on nucleoside transport in Sertoli cells, there are still many gaps in our current understanding. For example, previous studies have not localized nucleoside transporters to apical or basolateral membrane, nor have they demonstrated whether ENT1, ENT2, or both are responsible for basolateral nucleoside uptake. The purpose of this study is to address these questions. To accomplish this, we determined the kinetic and selectivity characteristics of transport of the representative nucleoside, uridine, in intact seminiferous tubules *ex vivo.* Primary cultured Sertoli cells were isolated from rat testis and also analyzed for

their ability to transport uridine. Immunohistochemical analysis was performed on both rat and human tissue to localize ENT1 and ENT2. These results support the conclusions that (i) rENT1 and hENT1 are located on the basolateral membrane of Sertoli cells; (ii) ENT1 is primarily responsible for basolateral nucleoside uptake into Sertoli cells; and (iii) rENT2 and hENT2 are localized to the apical membrane.

Methods

Materials: Quantigene HV Signal Amplification Kit and Quantigene Discovery Kit were purchased from Genospectra (Fremont, CA). Oligonucleotide probe sets for ENT1, ENT2, CNT1, and CNT2 were developed as published previously (Augustine et al, 2005). CNT3 sequence was obtained from GenBank and target sequences were analyzed by ProbeDesginer software version 1.0 (Genospectra, Fremont, CA). Probes were designed with a T_m of approximately 63°C, enabling hybridization conditions to be held constant at 53°C for each oligonucleotide probe set (Supplemental Table 1). Every probe developed through the ProbeDesigner software was BLAST-searched against the nucleotide database to ensure minimal or no cross-reactivity with other known rat sequences and expressed sequence tags. RNAzol B reagent was purchased from Tel-Test Inc. (Friendswood, TX) Non-radiolabeled uridine, DMEM/F12 media, tenofovir disoproxil fumarate (TDF), zidovudine (3'-azido-3'-deoxythymidine, AZT), and didanosine (2',3'-dideoxyinosine, ddI) were purchased from Sigma-Aldrich (St. Louis, MO). NBMPR was purchased from Santa Cruz Biotechnology Inc (Santa Cruz, CA). Stock solutions of NBMPR were made with DMSO. MACH4 IHC staining kit was acquired from Biocare Medical (St. Louis, MO). [^{3}H]uridine (specific activity: 30.1Ci/mMol) was purchased from American Radiolabeled Chemicals Inc (St. Louis, MO). ENT1 (SLC29A1) and the ENT2 (SLC29A2) rabbit antibodies were purchased from Lifespan Biosciences and quality was determined by the manufacturer (Seattle, WA). BD Matrigel Matrix and transwell inserts

used for primary Sertoli cell cultures were purchased from BD Biosciences (San Jose, CA). All other reagents were purchased from a standard scientific supplier at the highest available purity.

Branched DNA Assay: Specific oligonucleotide probes for ENT1, ENT2, CNT1, CNT2, and CNT3 were diluted in lysis buffer supplied by the Quantigene HV Signal Amplification Kit. Substrate solution, lysis buffer, capture hybridization buffer, amplifier, and label probe buffer used in the analysis were all obtained from the Quantigene Discovery Kit. The assay was performed in 96-well format with RNA isolated from seminiferous tubules added to the capture hybridization buffer and 50 µl of the diluted probe set. The total RNA was then allowed to hybridize to the probe set overnight at 53°C. Hybridization steps were performed per the manufacturer's protocol the following day. Luminescence of the samples was measured with a Quantiplex 320 bDNA luminometer interfaced with Quantiplex Data Management Software, version 5.02 (Bayer, Walpole, MA). Total RNA was isolated from rat seminiferous tubules or rat kidney tissue using RNAzol B reagent per the manufacturer's protocol. The integrity of the RNA was confirmed by ethidium bromide staining after agarose gel electrophoresis. Background for each transporter was determined using negative control wells which had all reagents except for RNA. The background was then subtracted to demonstrate expression above background levels.

Ex Vivo Transport Experiments with Intact Seminiferous Tubules: All protocols for obtaining animal tissue samples were approved by the University of Arizona Institutional Review Board (IRB) or Institutional Animal Care and Use Committee (IACUC). Seminiferous tubules were dissected from rat or mouse testes in chilled Ringer's solution containing (mM): 103 NaCl, 25 $NaHCO_3$, 19 sodium gluconate, 1 sodium acetate, 1.2 NaH_2PO_4, 5 KCl, 1 $CaCl_2$, 1 $MgCl_2$, and 5.5 glucose at pH 7.4. Images of the tubules were then taken for measurements of length needed to normalize the data. Uptake baths containing [^{3}H]uridine in Ringer's solution, alone or with varied concentrations of unlabeled uridine or NBMPR, were covered with oil to prevent

JPET Fast Forward. Published on May 2, 2013 as DOI: 10.1124/jpet.113.203265
This article has not been copyedited and formatted. The final version may differ from this version.

evaporation and brought to a temperature of 35° C. Individual tubules were transferred by a glass needle into the appropriate bath for a given period of time, and then transferred to wells containing 1 N NaOH for extraction of accumulated radioactivity, which was subsequently measured by an LS 6000 scintillation counter. At least three individual tubules were analyzed for each condition in all experiments. For studies using NBMPR, the concentration of DMSO was equal in all uptake baths and never exceeded 1 %.

Sertoli Isolation: Sertoli cell isolation was performed using the protocol of Mruk and Cheng, 2011. Briefly, the tunica was separated from the seminiferous tubules. Then the tubules were cut into 1mm pieces, incubated in 50/50 mixture of DMEM/F12 media, and resuspended in media with 0.002 % DNase and 0.1 % trypsin to release interstitial cells. After washing and resuspension, the media was replaced with a DMEM/F12 media with 1M glycine and 2 mM EDTA to lyse interstitial cells. The cells were resuspended in DMEM/F12 media with 0.1 % collagenase and 0.005 % DNase to remove the myoid layer. After washing, the cells were given fresh DMEM/F12 media with 0.1% hyaluronidase and 0.005 % DNase to break down the extracellular matrix. Cells were then plated at a density of 0.5 x 10^6 cells/cm^2 onto transwell inserts previously coated with a thin layer of Matrigel (diluted 1:7 with media) as per manufacturer's instructions (BD Biosciences). The cell media was supplemented with EGF and human transferin. After 36-48 hours at 37 ^{o}C, cells were treated with a 20 mM tris buffer (pH 7.4) for 2.5 minutes to lyse germ cells and then given fresh DMEM/F12 media supplemented with EGF and human transferin. Cells were then incubated at 37 $^{\circ}$C and cultured for an additional 4 days (6 days total from isolation). The media was changed as needed, typically every 1 to 2 days.

Primary Sertoli Cell Transport Experiments: Once the cells were confluent (day 6), the media was replaced with Waymouth Buffer containing (WB; mM): 135 NaCl, 13 HEPES, 2.5 $CaCl_2$, 1.2 $MgCl_2$•$6H_2O$, .8 $MgSO_4$•$7H_2O$, 5 KCl, 28 D-Glucose at pH 7.4. To measure basolateral-to-apical

transepithelial uridine flux, the cells were incubated at room temperature for 10 minutes before the buffer in the basolateral compartment was replaced with WB containing 1 µCi/mL of [^{3}H]uridine (approximately 30 nM) plus additional test agent (NBMPR, unlabeled uridine or NRTI drug) as required. At selected time intervals, WB from the apical compartment removed and assessed for radioactivity via liquid scintillation spectroscopy

To determine the rate of uridine transport across the basolateral membrane WB in the apical compartment was replaced with white paraffin oil. At 15 minutes, cells were lysed with 0.5 N NaOH, 1 % SDS solution for 20 minutes. The NaOH was neutralized using 1 N HCl. The radioactivity in the extract was measured by liquid scintillation spectroscopy. Each point represents an average of data collected in triplicate. For studies using NBMPR, the concentration for DMSO did not exceed 1 %.

Sample Collection: Animal samples were collected from euthanized rats either 21 days old (immature) or at least two months old (mature). The samples were fixed in 10% neutral buffered formalin overnight. A small incision was made in the tunica the next day and the samples remained in 10% neutral buffered formalin for another night. The following day, formalin was replaced with 70% ethanol until the samples were embedded in paraffin. Paraffin embedded human samples were purchased from the National Disease Research Interchange (NDRI) or were provided from the University of Arizona Medical Center pathology department. Patients had testis removed as part of therapy for prostate cancer. Human testis tissue was evaluated by a local pathologist and determined to be normal. Sectioning of all paraffin-embedded tissue was accomplished using a microtome with sections sliced 5 microns thick with one section per slide. Protocols for obtaining samples were approved by the University of Arizona Institutional Review Board (IRB) or Institutional Animal Care and Use Committee (IACUC).

Immunohistochemistry. IHC staining was performed on formalin-fixed, paraffin-embedded samples. Slides were deparaffinized with xylene and rehydrated with ethanol. The samples were then heated in an antigen retrieval buffer; citrate (pH 6.0) for ENT1, tris-EGTA (pH 9.0) for ENT2. Endogenous peroxide activity was blocked by a 0.3% hydrogen peroxide/methanol solution. Staining for ENT1 and ENT2 was performed with the MACH4 kit according to the manufacturer's instructions (Biocare Medical). All slides were imaged with a Leica DM4000B microscope and a DFC450 camera (Leica Microsystems Inc., Buffalo Grove, IL)

Statistics: Data are presented as means ±SE with the sample size representing separate experiments (each typically performed in triplicate). All tests of significance of observed differences were done by one-way analysis of variance using a Tukey *post hoc* multiple comparison test with $p < 0.05$ representing significance.

Results

Basolateral Uptake of [^{3}H]Uridine by Rodent Seminiferous Tubules: To analyze the role of ENT transporters in nucleoside transport across the BTB, we measured the ability of intact isolated single rodent seminiferous tubules to accumulate [^{3}H]uridine, thereby providing a measure of basolateral uptake. Figure 1 shows a time course for [^{3}H]uridine basolateral uptake in seminiferous tubules for rat (Figure 1A) and mouse (Figure 1B). The concentrations of [^{3}H]uridine in the bath were 0.41 µM for rat; 1.88 µM for mouse. Transport for both rat and mouse tubules was nearly linear for the first 5 minutes. Accumulation of [^{3}H]uridine into rat tubules was reduced by 54-83% over the first 20 minutes in the presence of 5 mM unlabeled uridine, suggesting that uridine uptake involved a saturable process.

The basolateral uptake of [^{3}H]uridine in both rat and mouse seminiferous tubules was inhibited by increasing concentrations of unlabeled uridine in a manner adequately described using the Michaelis-Menten equation for the competitive interaction of labeled and unlabeled substrate introduced by Malo and Berteloot (Malo and Berteloot, 1991). In five separate experiments K_t values for uridine transport were 314 ± 63 µM and 90 ± 24 µM, and J_{max} values were 2.5 ± 0.6 pmol/(min-mm) and 0.55 ± 0.2 pmol/(min-mm), for rat and mouse seminiferous tubules, respectively. Figure 2 shows the kinetic profiles for uridine uptake into these tubules, corrected for the non-saturable component of total uridine uptake.

Since uridine is commonly used as a substrate for ENT-mediated transport, it was anticipated that this process would be inhibited by NBMPR, a potent inhibitor of ENT1 and weak inhibitor of ENT2. The interaction between NBMPR and uridine transport is shown in Figure 3. The IC_{50} of NBMPR on [^{3}H]uridine was calculated by using the following equation (Groves et al, 1994):

JPET Fast Forward. Published on May 2, 2013 as DOI: 10.1124/jpet.113.203265
This article has not been copyedited and formatted. The final version may differ from this version.

$$J = \frac{J_{app}\,[\text{Uridine}^*]}{IC_{50} + [\text{NBMPR}]_o} + D\,[\text{Uridine}^*]$$

where J is the rate of [^{3}H]uridine uptake; J_{app} is the product of the maximum rate of [^{3}H]uridine uptake (J_{max}) and the ratio of the K_i of NBMPR and K_t for uridine transport; IC_{50} is the concentration of $[NBMPR]_o$ that reduced mediated (i.e., blockable) [^{3}H]uridine transport by 50%. The concentration of NBMPR was carried out to 500 nM, but maximal inhibition was achieved by 100 nM for both rats and mice. NBMPR inhibited this transport with an IC_{50} for the mediated (i.e. blockable) fraction of [^{3}H]uridine uptake of 23.6 ± 3.1 nM for rat tubules (Figure 3A) and 12.9 ± 0.7 nM for mouse tubules (Figure 3B). These IC_{50} values are similar to the range of IC_{50} values (0.1 nM to 68.5 nM) reported for ENT1 by others (Griffiths et al, 1997; Takano et al, 2010).

The 400 nM concentration of NBMPR did not appear to block uridine uptake into seminiferous tubules to the same extent as 5 mM unlabeled uridine (compare Fig 2 to Fig. 3 A, B). To compare the inhibition of NBMPR to that of unlabeled uridine, seminiferous tubules were categorized into four groups based on supplements in the media: control (no supplements), 5 mM uridine, 400 nM NBMPR, or 100 µM NBMPR (Figure 3C). The control group differed significantly from the other groups and there was also a significant difference between the 5 mM uridine and the 400 nM NBMPR groups. No significant difference was found between the other pairings. These data suggest that ENT2 plays no significant role in basolateral uridine transport, but that a small fraction (18.8%) of that accumulation may involve a pathway other than ENT1.

Basolateral Uptake of [^{3}H]Uridine by Primary Rat Sertoli Cells. To characterize the contribution of Sertoli cells to [^{3}H]uridine uptake by seminiferous tubules, primary Sertoli cells were isolated from rat testes and [^{3}H]uridine basolateral uptake was characterized on Matrigel-coated

transwell plates. Figure 4 shows a time course of basolateral-to-apical (transepithelial transport) of [^{3}H]uridine across primary cultured Sertoli cells. By 15 minutes, radiolabel appeared in the apical compartment. This signal was completely blocked at all time points by the addition of either 5 mM uridine, 100 nM NBMPR or 100 μM NBMPR.

Since ENT transporters are bidirectional, primary Sertoli cells were exposed to NBMPR and [^{3}H]uridine in the basolateral compartment followed by light paraffin oil application on the apical side (which prevents apical efflux of the hydrophilic uridine) to determine if inhibition of the transepithelial transport of [^{3}H]uridine was mediated by basolateral uptake or cellular efflux across the apical membrane. Figure 5 shows the 15 minute accumulation of [^{3}H]uridine into Sertoli cells across the basolateral membrane. That accumulation was reduced by 95% in the presence of 100 nM NBMPR, indicating that the inhibition of transepithelial transport seen in Figure 4 was due to the blocking of [^{3}H]uridine basolateral uptake into Sertoli cells.

mRNA Expression of Nucleoside Transporters in Fresh Seminiferous Tubules: In the light of evidence of CNT expression in primary cultured Sertoli cells (Kato et al, 2005), we determined mRNA expression of nucleoside transporters in freshly isolated rat seminiferous tubules, freshly isolated Sertoli cells, and primary Sertoli cells cultured for six days. Figure 6 shows branched DNA analysis of freshly isolated seminiferous tubules (6A) and primary Sertoli cells (6B). Expression of nucleoside transporters in seminiferous tubules was normalized to rat kidney tissue (which is known to express ENT1, ENT2, CNT1, CNT2, and CNT3) and expressed in relative light units (RLU) (Rodriguez-Mulero et al, 2005; Ishida et al, 2012). ENT1 expression was approximately 2.53 fold higher in seminiferous tubules than in kidney tissue. ENT2 expression was also highly expressed with RLU readings 0.94 compared to kidney. Expression of CNT1, CNT2, and CNT3 were much lower than that of ENT1 or ENT2 (0.05, 0.09, and .05 fold respectively).

In primary Sertoli cells, RLU values were normalized to GAPDH. ENT1 was found to be highly expressed (0.44 ± 0.14 and 0.35 ± 0.07 RLU for day 0 and day 6 respectively) as was ENT2 (0.75 ± 0.33 and 0.45 ± 0.12 for day 0 and day 6 respectively). Small amounts of CNT1 were detected (0.04 ± 0.01 and 0.04 ± 0.02 for both day 0 and day 6 respectively) but CNT2 and CNT3 expression were below background. No significant difference in transporter expression was observed between freshly isolated cells (day 0) and cells cultured for 6 days (day 6).

Immunohistochemical Staining of Rat and Human Testes. Immunohistochemical (IHC) staining for ENT1 and ENT2 was performed on rat testes to determine the subcellular distribution of these transporters. rENT1 and rENT2 were localized in Sertoli cells using IHC staining on both immature (Figure 7A, C) and mature (Figure 7B, D) rats. In both mature and immature testes, rENT1 was located on the basolateral membrane of Sertoli cells (Figure 7A, B). In contrast, slides stained for rENT2 expressed positive staining on the apical membrane but not on the basolateral membrane (Figure 7C, D).

IHC staining was also performed on adult human testes to determine if hENT1 and hENT2 share the same localization as their rat counterparts (Figure 8). Consistent with the expression profiles observed in rat testis, IHC staining revealed the presence of hENT1 on the basolateral membrane (Figure 8A), and hENT2 on the apical membrane (Figure 8B) of the Sertoli cells.

NRTI Inhibition of [^{3}H]Uridine Transport by Primary Cultured Rat Sertoli Cells. To determine whether the transporters used by uridine could also interact with NRTIs, transepithelial transport of uridine by primary Sertoli cells was measured in the presence of the NRTIs zidovudine (5 mM), didanosine (5 mM), and tenofovir disoproxil fumarate (1 mM). Each of these NRTIs significantly inhibited uridine transepithelial transport (Figure 9). The ability of these drugs to block basolateral uridine transport supports the contention that these NRTIs interact with the same transporter(s) used by uridine and may also act as substrates.

JPET Fast Forward. Published on May 2, 2013 as DOI: 10.1124/jpet.113.203265
This article has not been copyedited and formatted. The final version may differ from this version.

Discussion

We present a novel *ex vivo* technique for determining BTB transport using freshly isolated seminiferous tubules. Using both this novel *ex vivo* and traditional *in vitro* systems that employed 6 day cultured Sertoli cells, we demonstrated that, based on pharmacologic inhibition by NBMPR, basolateral uptake of nucleosides by Sertoli cells is dominated by ENT1. We also demonstrate that ENT2 does not play a significant role in basolateral uridine uptake into Sertoli cells. NBMPR inhibited 66% of total uridine uptake in rat seminiferous tubules at concentrations that pharmacologically inhibit ENT1 but do not affect ENT2 (100 nM) (Abd-Elfattah et al, 2012; Ward et al, 2000; Nishimura et al, 2012) (Fig. 3A, B). Of the saturable component (i.e. the portion of transport blocked by 5 mM unlabeled uridine), 400 nM NBMPR inhibited 81 % of uridine transport and increasing the NBMPR concentration to 100 μM (sufficient to block ENT2) did not result in a significant decrease in uridine uptake (Fig. 3C). This strongly implicates ENT1 as the primary transporter in nucleoside uptake into seminiferous tubules. The results with intact tubules were confirmed and extended by the observations in the primary cultured rat Sertoli cells. In these Sertoli cells, 100 nM NBMPR blocked the entire saturable portion of transepithelial uridine transport (Fig. 4), supporting the contention that transepithelial transport of uridine past the BTB depends on functional ENT1. Importantly, this inhibition was also observed in the basolateral uptake of uridine (Fig. 5), strongly supporting the conclusion that ENT1 mediates the basolateral entry for the transepithelial transport of uridine across Sertoli cells.

We also discovered that ENT2 is located on the apical membrane and not on the basolateral membrane. This is based on three observations. First, IHC data located ENT2 to the apical membrane but not to the basolateral membrane (Fig. 8). Second, inhibition of ENT1 (via 100 nM NBMPR) virtually stops all transepithelial transport of uridine across the basolateral membrane of Sertoli cells (Fig. 5). Third, increasing NBMPR concentration from 100 nM to 100 μM had little

further effect on inhibition of uridine uptake (Fig. 4, 5). These data demonstrate that ENT2 must play little to no role in basolateral uptake of uridine into seminiferous tubules.

Interestingly, in seminiferous tubules, there was a small portion (approximately 19%) of [^{3}H]uridine transport that was blocked by unlabeled uridine but not by high concentrations of NBMPR. Since NBMPR can prevent transport of uridine in Sertoli cells, this unexplained accumulation may not reflect activity of Sertoli cells. Perhaps it is due to some effect of the myoid layer which is removed during Sertoli cell isolation. However, because such a large proportion of uptake into the tubules is blocked by 100 nM NBMPR (which has no effect on CNT-mediated transport), ENT1 seems to be the primary transporter responsible for nucleoside uptake into seminiferous tubules. This is in agreement with expression of ENT1 but not ENT2 on the basolateral membrane of Sertoli cells. The identical localizations of ENT1 and ENT2 in both rat and human tissues suggest that data gathered from rat Sertoli cells and seminiferous tubules may be applicable to humans. Unfortunately, fresh human seminiferous tubules were unavailable so uptake studies with human seminiferous tubules could not be performed.

We also demonstrated through branched DNA analysis that ENTs are the primary nucleoside transporters expressed in fresh seminiferous tubules, fresh Sertoli cells, and 6 day cultured primary Sertoli cells all had low to undetectable expression of CNTs (Figure 6). Furthermore, the complete inhibition of basolateral uridine uptake produced by 100 nM NBMPR suggests that CNTs do not exert an appreciable impact on basolateral transport of uridine in Sertoli cells (Figure 4, 5). This would indicate that any CNTs expressed by Sertoli cells, which bDNA analysis suggests being very modest, would be localized to the apical membrane.

Whereas the function of ENT1 on the basolateral membrane is evident, the role of ENT2 on the apical membrane is less clear. A common physiological function of ENT transporters is to transport nucleosides from the blood into the cell and this is how we believe ENT1 functions in

Sertoli cells (Kato et al, 2005; Molina-Arcas et al, 2008). As ENT1 transports nucleosides into the cell, the intracellular concentration of these molecules could rise to approach that in the blood. Since ENT transporters move nucleosides according to their concentration gradient, ENT2 on the apical membrane would transport nucleosides from inside the cell into the lumen of the seminiferous tubule where they can be used by developing germ cells. These dividing germ cells could act as a 'nucleoside sink' keeping the luminal nucleoside concentration low enough to drive unidirectional transport. Figure 10 provides an illustration of how this hypothesized process could be functioning to transport nucleosides into the lumen. To the extent that CNTs are expressed in the apical membrane of Sertoli cells, their activity would be expected to reabsorb some fraction of nucleoside secreted by ENT2. Since we suspect that CNTs impact on nucleoside transport into native Sertoli cells is likely to be minimal (see earlier discussion), we do not expect these transporters to have a substantial impact on nucleoside transport. Clearly, more studies involving ENT2 and CNTs on the apical membrane of Sertoli cells are required to verify this model.

Using this model, if the NRTI concentration inside the seminiferous tubules rose above that of the blood, then ENT2 and ENT1 would remove drug from the tubules and transport it back into the blood. This would suggest that the concentration of NRTI drugs would never rise above that of the blood in the seminiferous tubule. This is puzzling since clinical data has indicated that NRTI drugs are up to 10 fold more concentrated in seminal plasma than in blood plasma (Dumond *et al*, 2008). One possible explanation could be that NRTI drugs reach concentrations similar to blood levels in the seminiferous tubules, but are then concentrated further down the male genital tract (MGT). Fluid from the seminiferous tubule flows into the epididymis where up to 99% of the water can be reabsorbed (Lu, 2008; Cornwall, 2009). Assuming drug is not also reabsorbed, this would increase the concentration of drug approximately 100 fold. During ejaculation, drug from the epididymis would mix with secretions from accessory sex organs

(primarily secretions originating from the seminal vesicles and prostrate) resulting in dilution of the drug (Van Praag et al, 2001; Cao et al, 2008; Caballero et al, 2012). Since testicular fluid has been estimated to contribute up to 10% of the total volume for semen, this would dilute the drug to roughly 10 fold above blood concentration (Van Praag et al, 2001). This illustrates a possible mechanism for drugs crossing the BTB and then becoming concentrated in the MGT resulting in a higher concentration of drug in the seminal plasma than in blood plasma.

The assumption that drug is not reabsorbed in the epididymis requires further investigation. Studies investigating epididymal drug transport are limited. However, one study revealed that ENT1, ENT2, and CNT2 are present in the epididymis (Leung et al, 2001). Without knowing the localization of these transporters, it is difficult to speculate on their potential impact on drug transport. If, for example, CNT2 is the only nucleoside transporter on the apical membrane, then pyrimidine-based analogs, such as zidovudine and lamivudine, would not be reabsorbed since CNT2 transports purine-based analogs (Van Aubel et al, 2000; Gray et al, 2004;).

This ENT dominant system is a possible mechanism for NRTI transport at the BTB. We showed that ENTs are localized in Sertoli cells in a manner that would support transepithelial transport, ENT1 is necessary for basolateral nucleoside transport, and some NRTIs can inhibit transepithelial transport of uridine, which indicates that they interact with the same transporters (Figure 9). This is in agreement with other sources which have demonstrated that ENT transporters can transport NRTIs (Ward et al, 2000). Taken together, these data indicate the possibility of a novel ENT-mediated pathway for the penetration of nucleosides and NRTIs past the BTB.

JPET Fast Forward. Published on May 2, 2013 as DOI: 10.1124/jpet.113.203265
This article has not been copyedited and formatted. The final version may differ from this version.

Acknowledgements

We would like to thank the NIH-funded National Disease Research Interchange and Rob Klein (University of Arizona Medical Center) for providing paraffin-embedded human samples.

Authorship contributions

Participated in research design: Klein, Evans, Hardwick, Dantzler, Wright, and Cherrington

Conducted experiments: Klein and Evans

Contributed new reagents or analytical tools: Evans

Performed data analysis: Klein, Evans, Hardwick, Dantzler, Wright and Cherrington

Wrote or contributed to the writing of the manuscript: Klein, Dantzler, Wright and Cherrington

References

Abd-Elfattah AS, Ding M, Jessen ME and Wechsler AS (2012) On-pump inhibition of es-ENT1 nucleoside transporter and adenosine deaminase during aortic crossclamping entraps intracellular adenosine and protects against reperfusion injury: Role of adenosine A1 receptor. *J Thorac Cardiovasc Surg*. doi:10.1016/j.jtcvs.2011.09.073

Anderson PL, Noormohamed SE, Henry K, Brundage RC, Balfour HH, Jr. and Fletcher CV (2000) Semen and serum pharmacokinetics of zidovudine and zidovudine-glucuronide in men with HIV-1 infection. *Pharmacotherapy* 20:917-922.

Augustine LM, Markelewicz RJ, Jr., Boekelheide K and Cherrington NJ (2005) Xenobiotic and endobiotic transporter mRNA expression in the blood-testis barrier. *Drug Metab Dispos* 33:182-189.

Baldwin SA, Beal PR, Yao SY, King AE, Cass CE and Young JD (2004) The equilibrative nucleoside transporter family, SLC29. *Pflugers Arch* 447:735-743.

Byrn RA and Kiessling AA (1998) Analysis of human immunodeficiency virus: indications of a genetically distinct virus reservoir *Am J Reprod Immunol* 41:161-176

Caballero I, Parrilla I, Alminana C, D el Olmo, Roca J, Martinez EA, and Vasquez JM (2012) Seminal plasma proteins as modulators of the sperm function and their application in sperm biotechnologies. *Reprod Dom Anim* 47:12-21

Cao YJ, Caffo B, Choi L, Radebaugh CL, Fuch EJ, Hendrix CW (2008) Noninvasive quantification of drug concentration in prostate and seminal vesicles: improvement and validation with desipramine and asprin. *J Clin Pharmacol* 48:176-183

Cornwall GA (2009) New insights into epididiymal biology and function *Hum Reprod* 15:213-227

Dahl V, Josefsson L and Palmer S (2010) HIV reservoirs, latency, and reactivation: Prospects for eradication *Antiviral Res.* 85:286-294

Dumond JB, Reddy YS, Troiani L, Rodriguez JF, Bridges AS, Fiscus SA, Yuen GJ, Cohen MS and Kashuba AD (2008) Differential extracellular and intracellular concentrations of zidovudine and lamivudine in semen and plasma of HIV-1-infected men. *J Acquir Immune Defic Syndr* 48:156-162.

Else LJ, Taylor S, Back DJ and Khoo SH (2011) Pharmacokinetics of antiretroviral drugs in anatomical sanctuary sites: the male and female genital tract. *Antivir Ther* 16:1149-1167

Errasti-Murugarren E, Fernández-Calotti P, Veyhl-Wichmann M, Diepold M, Pinilla-Macua I, Pérez-Torras S, Kipp H, Koepsell H, Pastor-Anglada M. (2012) Role of the transporter regulator protein (RS1) in the modulation of concentrative nucleoside transporters (CNT2) in epithelia. *Mol Pharmacol* 82 (1): 59-67

Fernandez-Calotti PX, Colomer D, and Pastor-Anglada M (2011) Translocation of nucleoside analogs across the plasma membrane in hematologic malignancies. *Nucleosides, Nucleotides and Nucleic acids* 30:1324-1340

Gray JH, Owen RP, Giacomini KM (2004) The concentrative nucleoside transporter family, SLC28. *Eur J Phy* 447:728-734

Griffiths M, Yao SY, Abidi F, Phillips SE, Cass CE, Young JD, and Baldwin SA (1997) Molecular cloning and characterization of a nitrobenzylthioinosine-insensitive (*ei*) equilibrative nucleoside transporter from human placenta. *Biochem J* 328:739-743.

Groves CE, Evans KK, Dantzler WH, and Wright SH (1994) Peritubular organic cation transport in isolated rabbit proximal tubules. *Am J Physiol* 266:F450-458Ishida K, Fukao M, Watanabe H, Taguchi M, Miyawaki T, Matsukura H, Uemura O, Zhang Z, Unadkat JD and Hashimoto Y (2012) Effect of salt intake on bioavailability of mizoribine in healthy Japanese males. *Drug Metab Pharmcokinet* doi 10.2133/dmpk.DMPK-12-NT-043

Kato R, Maeda T, Akaike T and Tamai I (2005) Nucleoside transport at the blood-testis barrier studied with primary-cultured sertoli cells. *J Pharmacol Exp Ther* 312:601-608.

Kato R, Maeda T, Akaike T, Tamai I (2009) Characterization of nucleobase transport by mouse Sertoli cell line TM4. *Biol Pharm Bull* 32(3):450-455.

Kong W, Engel K and Wang J (2004) Mammalian nucleoside transporters *Curr Drug Metab* 5:63-84

Leung GP, Ward JL, Wong PY, and Tse CM (2001) Characterization of nucleoside transport systems in cultured rat epididymal epithelium. *Am J Physiol* 280:C1076-C1082

Li N, Wang T, Han D, (2012) Structural, cellular and molecular aspects of immune privilege in the testis. *Front Immunol* 3:152

Lu DY, Li Y, Bi ZW, Yu HM and Li XJ (2008) Expression and immunohistochemical localization of aquaporin-1 in male reproductive organs of the mouse. *Anat. Histol. Embryol.* 37:1-8

Lu H, Chen C and Klaassen C (2004) Tissue distribution of concentrative and equilibrative nucleoside transporters in male and female rats and mice. *Drug Metab Dispos* 32:1455-1461

Malo C and Berteloot A (1991) Analysis of kinetic data in transport studies: new insights from kinetic studies of Na(+)-D-glucose cotransport in human intestinal brush-border membrane vesicles using a fast sampling, rapid filtration apparatus. *Membr Biol* 122(2):127-41

Mital P, Hinton BT and Dufour JM (2011) The blood-testis and blood-epididymis barriers are more than just their tight junctions. *Biol Reprod* 84:851-858.

Molina-Arcas M, Trigueros-Motos L, Casado FJ and Pastor-Anglada M (2008) Physiological and pharmacological roles of nucleoside transporter proteins. *Nucleosides Nucleotides Nucleic Acids* 27:769-778.

Mruk DD and Cheng CY (2011) An in vitro system to study Sertoli cell blood-testis barrier dynamics. *Methods Mol Biol* 763:237-252.

Nishimura T, Chishu T, Tomi M, Nakamura R, Sato K, Kose N, Sai Y, Nakashima E (2012) Mechanism of nucleoside uptake in rat placenta and induction of placental CNT2 in experimental diabetes *Drug Metab Pharmcokinet* doi:10.2133/dmpk.DMPK-11-RG-103

Olson DP, Scadden DT, D'Aquila RT, De Pasquale MP, (2002) The protease inhibitor ritonavir inhibits the functional activity of the multidrug resistance related-protein 1 (MRP-1) *AIDS* 16:1743-1747

Pastor-Anglada M, Cano-Soldado P, Molina-Arcas M, Lostao MP, Larráyoz I, Martínez-Picado J, Casado FJ (2005) Cell entry and export of nucleoside analogues. *Virus Res* 107:151-164

Pelletier RM (2011) The blood-testis barrier: the junctional permeability, the proteins and the lipids. *Prog Histrochem Cyto* 46(2): 49-127

Pereira AS, Smeaton LM, Gerber JG, Acosta EP, Snyder S, Fiscus SA, Tidwell RR, Gulick RM, Murphy RL and Eron JJ, Jr. (2002) The pharmacokinetics of amprenavir, zidovudine, and lamivudine in the genital tracts of men infected with human immunodeficiency virus type 1 (AIDS clinical trials group study 850). *J Infect Dis* 186:198-204.

Prins JM, Lowe SH, van Leeuwen E, Droste JA, van der Veen F, Reiss P, Lange JM, Burger DM, Repping S (2007) Semen quality and drug concentrations in seminal plasma of patients using a didanosine or didanosine plus tenofovir containing antiretroviral regimen.*Ther Drug Monit* 29(5): 566-570

Ritzel MW, Ng AM, Yao SY, Graham K, Loewen SK, Smith KM, Ritzel RG, Mowles DA, Carpenter P, Chen XZ, Karpinski E, Hyde RJ, Baldwin SA, Cass CE, Young JD. (2000) Molecular identification and characterization of novel human and mouse concentrative Na^+ nucleoside cotransporter proteins (hCNT3 and mCNT3) broadly selective for purine and pyrimidine nucleosides *J Biol Chem* 276(**4**):2914-27

Rodriguez-Mulero S, Errasti-Murugarren E, Ballarin J, Felipe A, Doucet A, Casado FJ, and Pastor-Anglada M. (2005) Expression of concentrative nucleoside transporters SLC28 (CNT1, CNT2, and CNT3) along the rat nephron: Effect of diabetes *Kidney Int* 68, 665–672.

Takano M, Kimura E, Suzuki S, Nagai J, and Yumoto R (2010) Human erythrocyte nucleoside transporter 1 ENT1 functions at ice cold temperatures. *Drug Metabl Pharmacokinet* 25(4):351-360

Van Aubel RA. Masereeuw R, and Russel FG (2000) Molecular pharmacology of renal organic anion transporters. *Am J Physiol* 279:F216-F232

Van Praag RM, Repping S, de Vries JW, Lange JM, Hoetelmans RM, Prins JM (2001) Pharmacokinetic profiles of nevirapine and indinavir in various fractions of seminal plasma. *Antimicrob Agents Chemother* 45(10): 2902-2907.

Ward JL, Sherali A, Mo ZP, and Tse CM (2000) Kinetic and pharmacological properties of cloned human equilibrative nucleoside transporters, ENT1 and ENT2, Stably Expressed in Nucleoside Transporter-deficient PK15 Cells. *J. Biol. Chem.*275: 8375-8381

Yao SY, Ng AM, Cass CE, Baldwin SA, and Young JD (2011) Nucleobase transport by human equilibrative transporter 1 (hENT1) *J Biol Chem* 286:32552-32562

Footnotes

This work was supported by the National Institutes of Health [Grants NIAID AI083927, ES006694, and HD062489].

JPET Fast Forward. Published on May 2, 2013 as DOI: 10.1124/jpet.113.203265
This article has not been copyedited and formatted. The final version may differ from this version.

Figure Legends

Figure 1. **Time course of basolateral transport of [^{3}H]uridine by rodent seminiferous tubules**. Composite graphs depicting [^{3}H]uridine transport by rat (A) or mouse (B) intact seminiferous tubules through the basolateral surface over time. The mean concentration of [^{3}H]uridine in the baths were 0.41 µM and 1.88 µM for rats and mice, respectively. [^{3}H]uridine transport in the presence of 5 mM unlabeled uridine was analyzed to determine the saturable portion of uridine transport in rat seminiferous tubules. The insets demonstrate the saturable uptake of rat or mouse seminiferous tubules at 5 minutes with and without the presence of 5 mM uridine. Each point represents the mean (±standard error) of four experiments for rats and two experiments for mice (±half the range), each with a different animal. At least three tubules per time point were analyzed in each experiment.

Figure 2. ***Ex vivo*** **kinetic analysis of basolateral transport of [^{3}H]uridine by rodent seminiferous tubules.** Composite graphs demonstrating basolateral [^{3}H]uridine transport by rat (A) or mouse (B) intact seminiferous tubules in the presence of increasing concentrations of unlabeled uridine. The mean concentrations of [^{3}H]uridine in the baths were 0.45 µM and 0.37 µM for rats and mice, respectively. K_t values were calculated to be 314 µM and 90 µM for rat and mouse seminiferous tubules, respectively. Each point represents an average (±standard error) of at least five different experiments, each with a different animal. At least three separate tubules for each unlabeled uridine concentration were analyzed in each experiment.

Figure 3. ***Ex vivo*** **analysis of the effects of NBMPR on basolateral transport of [^{3}H]uridine by rodent seminiferous tubules**. Composite graphs depicting [^{3}H]uridine transport by rat (A) or mouse (B) intact seminiferous tubules in the presence of increasing concentrations of NBMPR. The mean concentrations of [^{3}H]uridine in the baths were 0.43 µM and 1.11 µM for rats and mice, respectively. IC_{50} values were calculated to be 23.6 nM and 12.9 nM for rat and mouse

seminiferous tubules, respectively. Each point represents an average (±standard error) of at least five experiments, each with a different animal. At least three separate tubules for each NBMPR concentration were analyzed in each experiment.

The bar graph (C) represents *ex vivo* basolateral uptake of [^{3}H]uridine in intact rat seminiferous tubules. The mean concentration of [^{3}H]uridine in the baths was 45 µM. Control represents [^{3}H]uridine uptake in the absence of NBMPR or unlabeled uridine. [^{3}H]uridine transport in the presence of 5mM unlabeled uridine was analyzed to determine the saturable portion of uridine transport. The concentrations of NBMPR are enough to block just ENT1 activity (400 nM) or both ENT1 and ENT2 (100 µM). The height of each bar is 6.22 (control), 1.12 (5 mM uridine), 2.08 (400 nM NBMPR), and 1.55 (100 µM NBMPR) fmols mm^{-1} min^{-1}. Asterisks (*) indicate significance ($p < 0.05$) compared to control whereas the dagger (□) indicates significance ($p < 0.05$) compared to 400 nM NBMPR.

Figure 4. ***In vitro*** **analysis of role of rENT1 and rENT2 in [^{3}H]uridine transepithelial transport by primary cultured Sertoli cells**. Confluent monolayers of primary cultured rat Sertoli cells were exposed to 40 nM [^{3}H]uridine in the basolateral compartment. Apical media was counted to determine transepithelial transport. Cells were exposed to concentrations of NMBPR sufficient to inhibit ENT1 (100 nM), ENT2 and ENT1 (100 µM), or unlabeled uridine (5 mM). Control cells were not given NBMPR or unlabeled uridine. The lines describing the data were fit by eye. Each point represents an average (±standard error) of triplicate wells of Sertoli cells derived from a mixture of three rats.

Figure 5. **Effects of NBMPR on the basolateral uptake of [^{3}H]uridine in primary cultured rat Sertoli cells.** Confluent monolayers of primary cultured rat Sertoli cells were provided with 40 nM [^{3}H]uridine in the basolateral compartment. After 15 minutes, cells were lysed and the lysates were counted to determine cellular accumulation of [^{3}H]uridine. Cells were exposed to

concentrations of NBMPR sufficient to inhibit ENT1 uptake (100 nM), ENT2 and ENT1 (100 μM), or unlabeled uridine (5 mM). Control cells were not given NBMPR or unlabeled uridine. Each point represents an average (± half the range) of duplicate wells of Sertoli cells derived from a mixture of three rats. The height of each bar is 26.81 (control), 1.33 (5 mM uridine), 0.53 (400 nM NBMPR), and 0.34 (100 μM) fmol mm^{-1} min^{-1}.

Figure 6. **Branched DNA analysis of nucleoside transporter expression in seminiferous tubules relative to kidney.** RNA extracted from freshly isolated seminiferous tubules or kidney tissue (A) from 4 rats was analyzed for expression of ENT1, ENT2, CNT1, CNT2, and CNT3. To account for variations among probe sets, expression of each transporter was compared to kidney as a positive control. Graph depicts above background expression relative to positive control. Results show that expression for ENT1 253.9%, ENT2 94.0%, CNT1 5.2%, CNT2 9.3% and CNT3 5.2% relative to kidney expression. Each point represents the mean (±standard error) of 6 wells.

RNA was also extracted from freshly isolated Sertoli cells or 6 day cultured Sertoli cells (B) from 4 rats was also analyzed for expression of ENT1, ENT2, CNT1, CNT2, and CNT3. All RLU values were normalized to GAPDH expression. RLU values freshly isolated primary Sertoli cells (day 0) were: ENT1 0.44, ENT2 0.75, CNT1 0.04, CNT2 0.02, and CNT3 0.01. For cultured primary Sertoli cells (day 6) were: ENT1 0.35, ENT2 0.46, CNT1 0.04, CNT2 0.01 and CNT3 0.03. Each point represents the mean (±standard error) of 3 wells.

Figure 7. **Localization of rENT1 and rENT2 in the testis.** Immunohistochemical staining for ENT1 (A, B) or ENT2 (C, D) in formalin-fixed paraffin-embedded immature (A, C) or mature (B, D) rat testes is shown at 40 X magnification. Arrows indicate positive (brown) staining for proteins. L indicates lumen of seminiferous tubules.

Figure 8. **Localization of hENT1 and hENT2 in the testis** Immunohistochemical staining for ENT1 (A) or ENT2 (B) in formalin-fixed paraffin-embedded adult human testes is shown at 40 X magnification. Arrows indicate positive (brown) staining for proteins. L indicates lumen of seminiferous tubules.

Figure 9. **Inhibition of [^{3}H]uridine transport by NRTI in primary cultured rat Sertoli cells.** Confluent monolayers of primary cultured rat Sertoli cells were exposed to media in the basolateral compartment containing 40 nM [^{3}H]uridine and either zidovudine (5 mM), didanosine (5mM), or tenofovir disoproxil fumarate (1 mM). Control wells were not exposed to any NRTI drugs. Media from the apical compartments were counted to assess transepithelial transport of [^{3}H]uridine after 15 minutes. Each bar represents an average (±standard error) of triplicate wells of Sertoli cells derived from a mixture of three rats. The height of each bar is 27.52 (control), 11.52 (zidovudine), 9.51 (didanosine), and 13.79 (tenofovir disoproxil fumarate). Asterisks (*) indicate significance ($p < 0.05$) compared to control.

Figure 10. **Model of ENT-Mediated Transport of Nucleosides Across the BTB.** An illustration of the seminiferous tubule and surrounding cells depicting how nucleosides could be transported into the lumen via ENT transporters. ENT1 is the primary transporter responsible for uptake of nucleosides into the Sertoli cells due to the higher concentration of nucleosides in the blood. ENT2 is proposed to play a role in efflux of nucleosides into the lumen of the seminiferous tubules due to the higher concentration of intracellular nucleosides (mediated by ENT1) compared to the lumen of the seminiferous tubule.

Figure 1

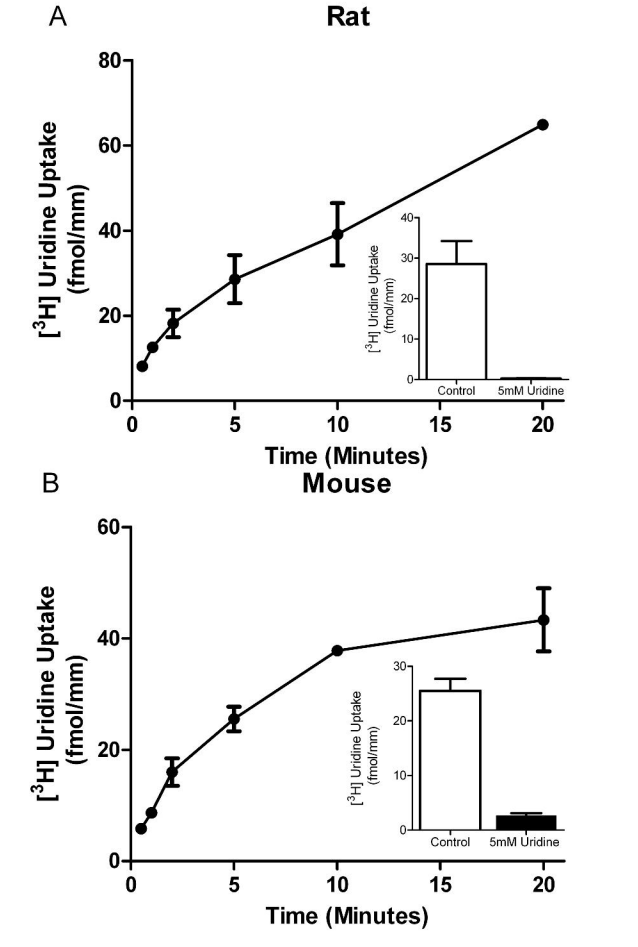
A
Rat
[3H] Uridine Uptake (fmol/mm)
80
60
40
20
0
0
5
10
15
20
Time (Minutes)
[3H] Uridine Uptake (fmol/mm)
40
30
20
10
0
Control
5mM Uridine
B
Mouse
[3H] Uridine Uptake (fmol/mm)
60
40
20
0
0
5
10
15
20
Time (Minutes)
[3H] Uridine Uptake (fmol/mm)
30
20
10
0
Control
5mM Uridine

Figure 2

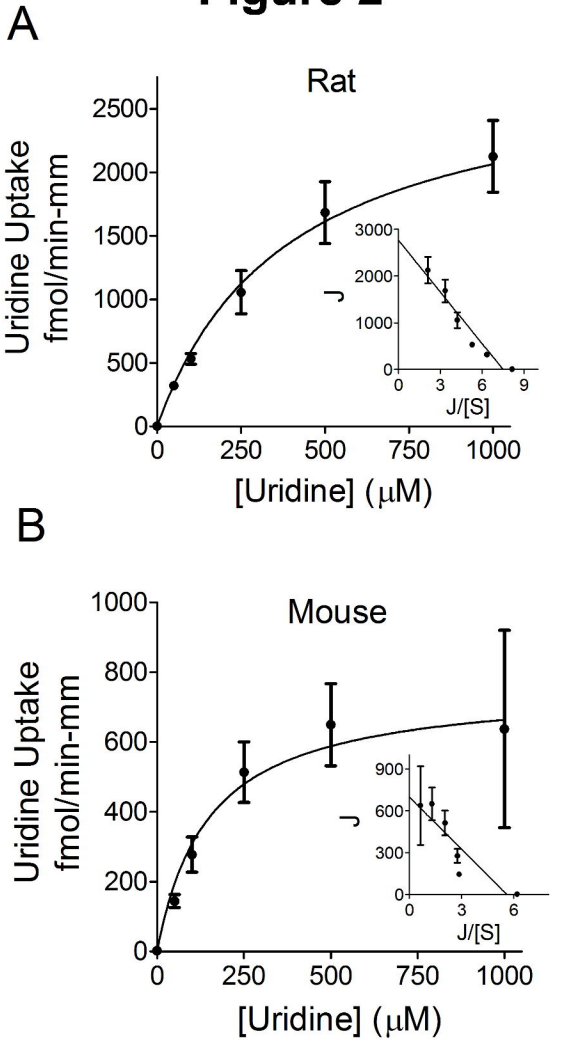
A
Rat
Uridine Uptake
fmol/min-mm
2500
2000
1500
1000
500
0
0
250
500
750
1000
[Uridine] (μM)
J
3000
2000
1000
0
0
3
6
9
J/[S]
B
Mouse
Uridine Uptake
fmol/min-mm
1000
800
600
400
200
0
0
250
500
750
1000
[Uridine] (μM)
J
900
600
300
0
0
3
6
J/[S]

Figure 3

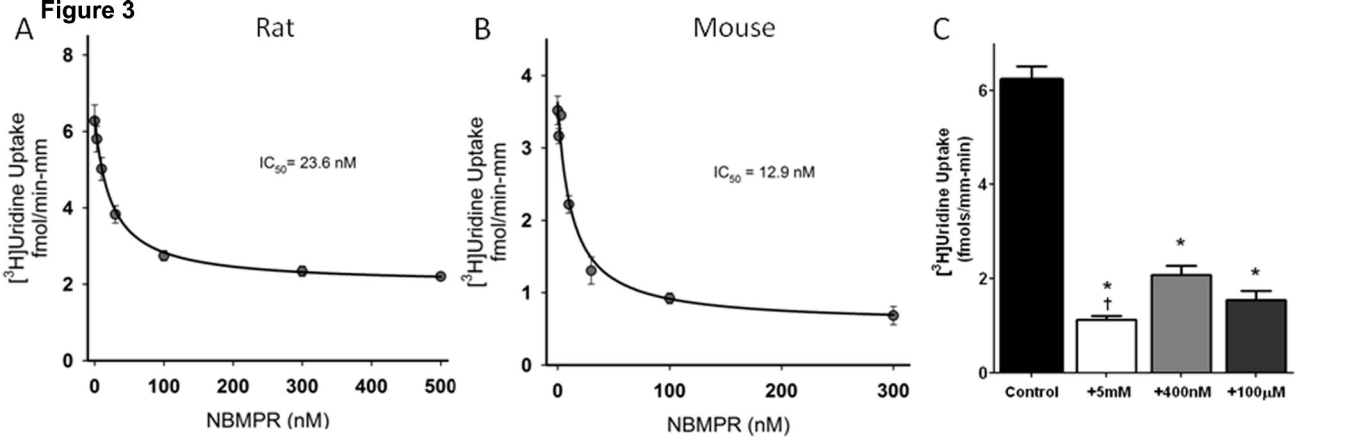
A
Rat
[3H]Uridine Uptake fmol/min-mm
IC50= 23.6 nM
NBMPR (nM)
B
Mouse
[3H]Uridine Uptake fmol/min-mm
IC50 = 12.9 nM
NBMPR (nM)
C
[3H]Uridine Uptake (fmols/mm-min)
Control
+5mM
+400nM
+100μM

Figure 4

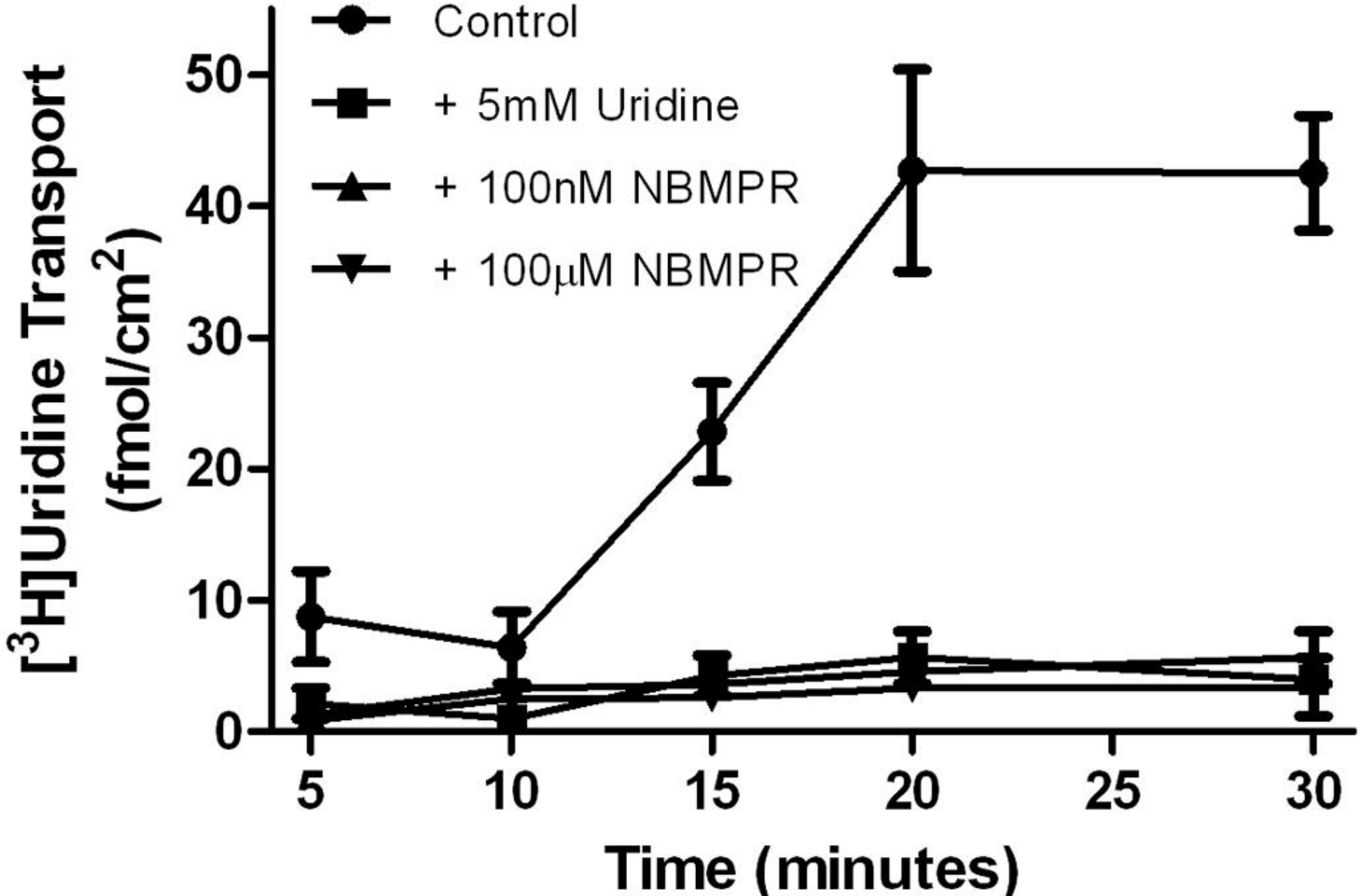
Control
+ 5mM Uridine
+ 100nM NBMPR
+ 100μM NBMPR
[3H]Uridine Transport
(fmol/cm2)
0
10
20
30
40
50
5
10
15
20
25
30
Time (minutes)

Figure 5

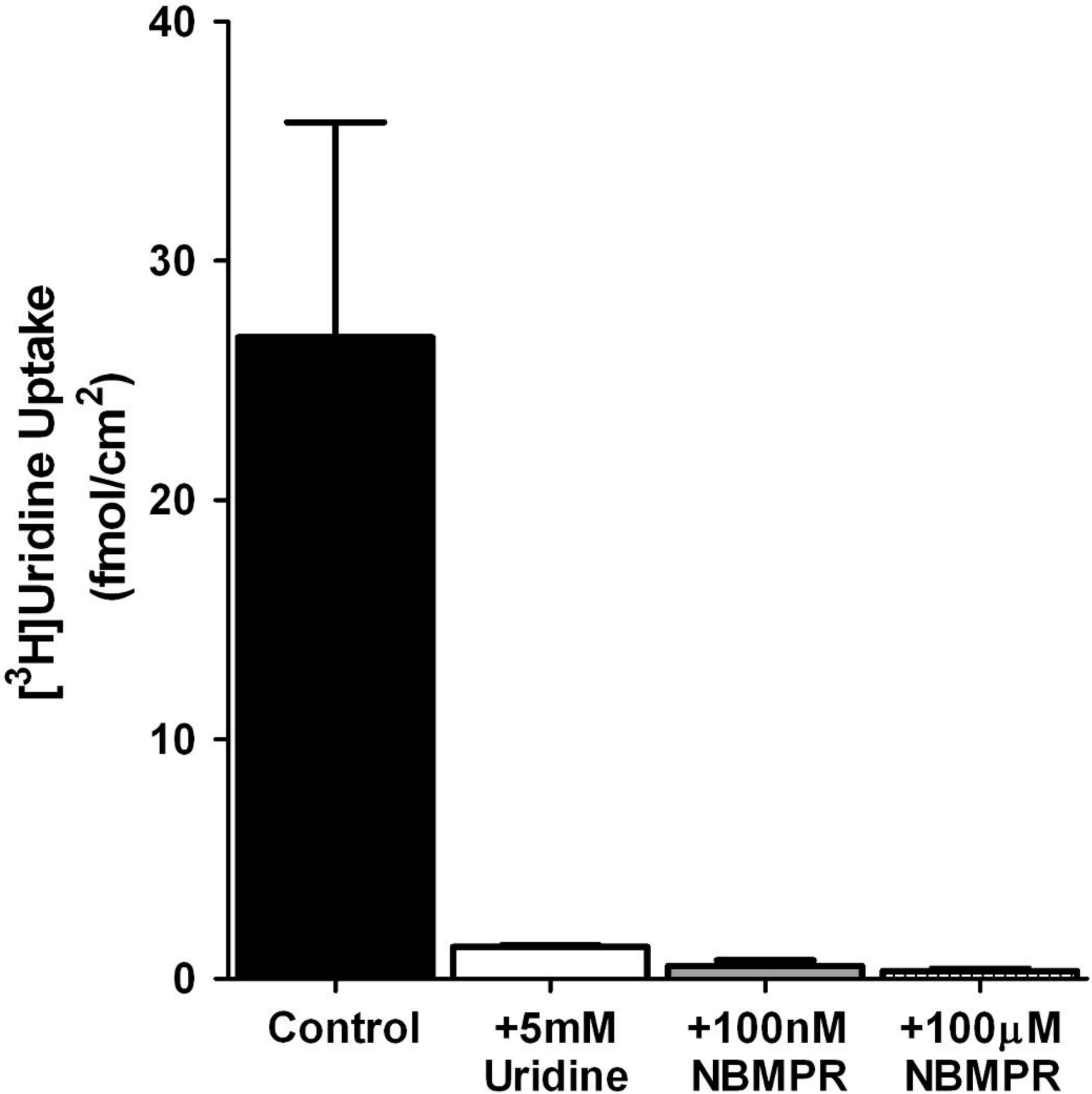
40
30
20
10
0
[3H]Uridine Uptake
(fmol/cm2)
Control
+5mM
Uridine
+100nM
NBMPR
+100μM
NBMPR

Figure 6

A

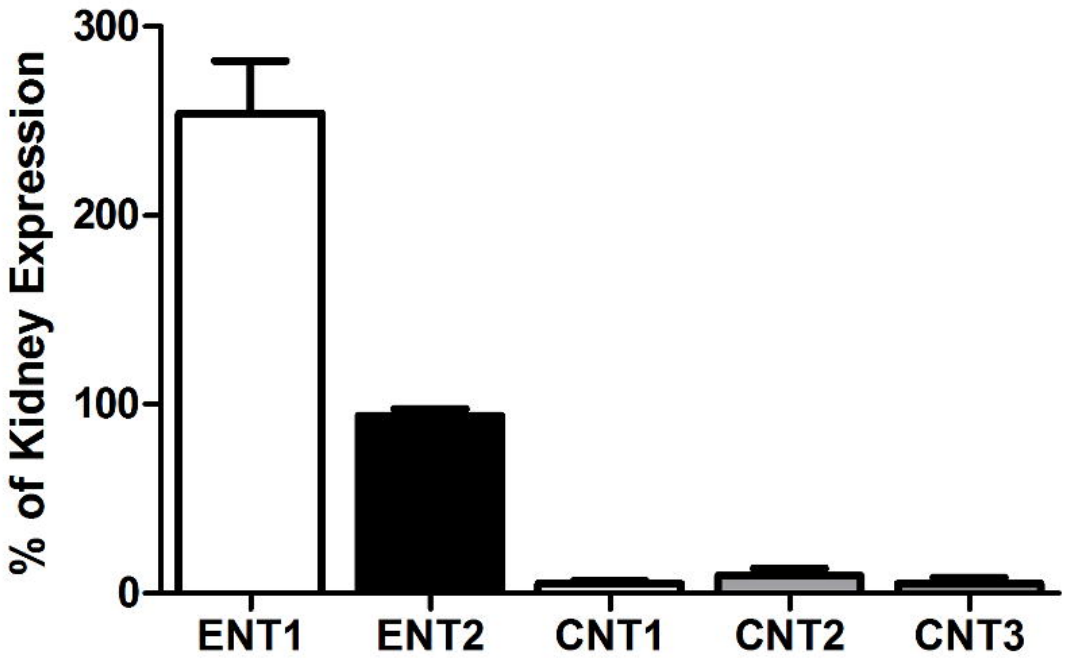
% of Kidney Expression
300
200
100
0
ENT1
ENT2
CNT1
CNT2
CNT3

B

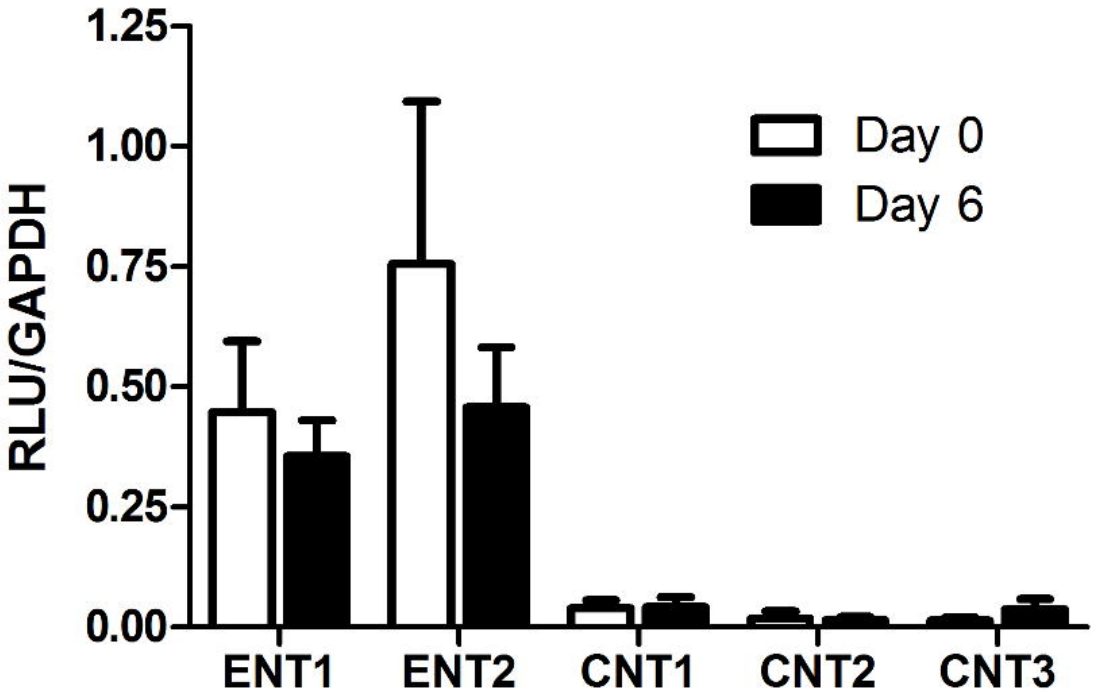
RLU/GAPDH
1.25
1.00
0.75
0.50
0.25
0.00
Day 0
Day 6
ENT1
ENT2
CNT1
CNT2
CNT3

Figure 7

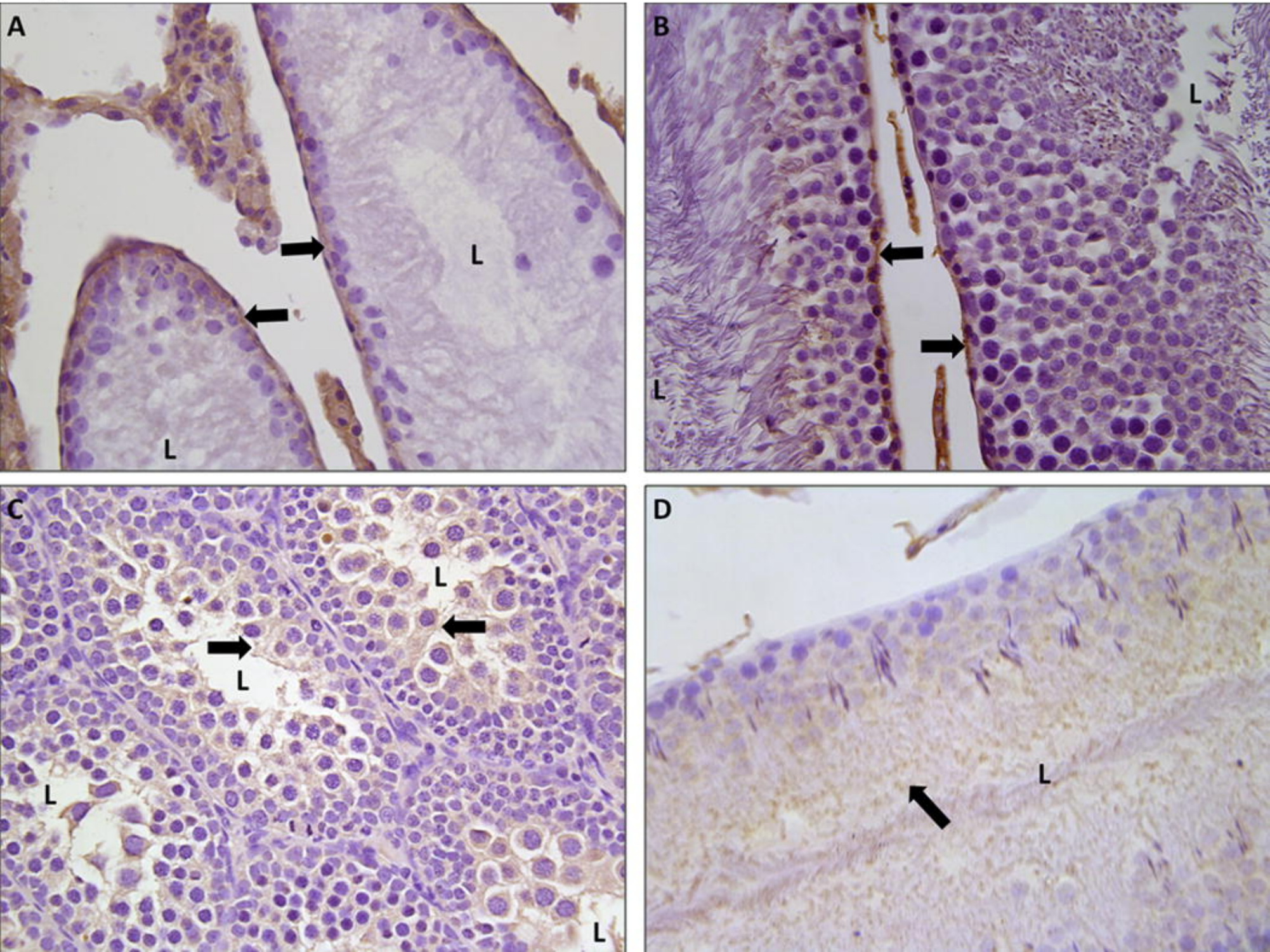

Figure 8

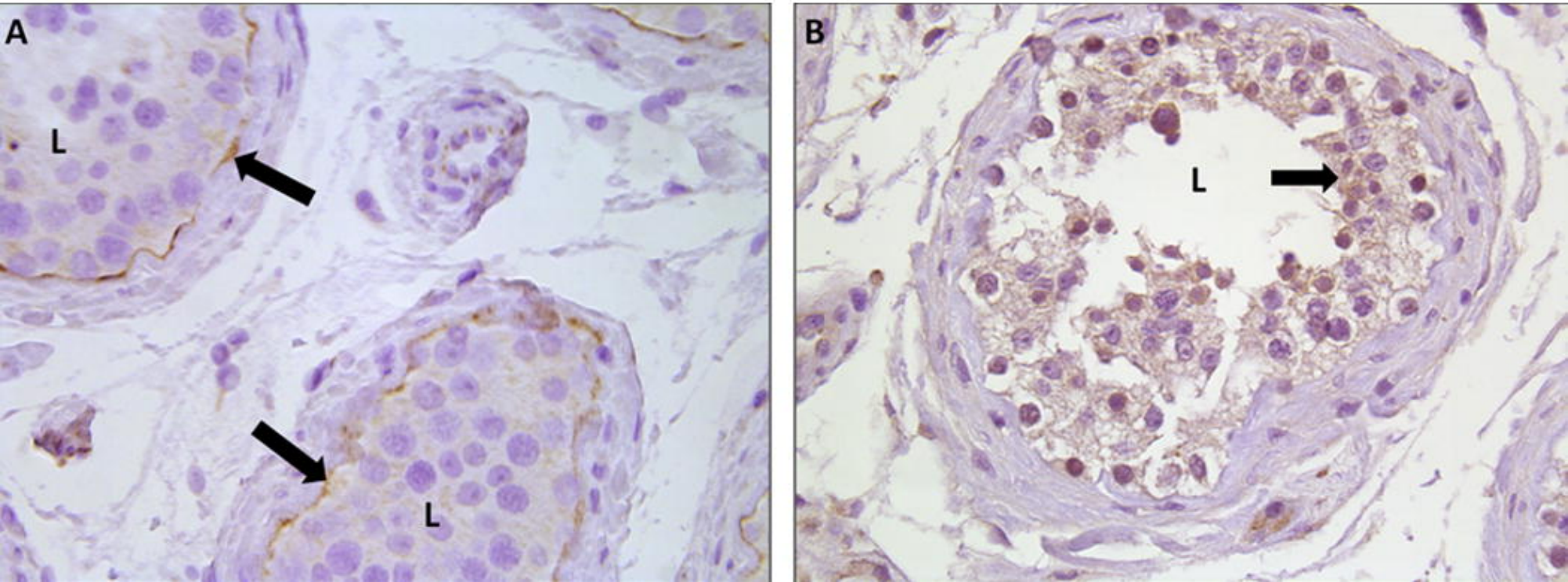

Figure 9

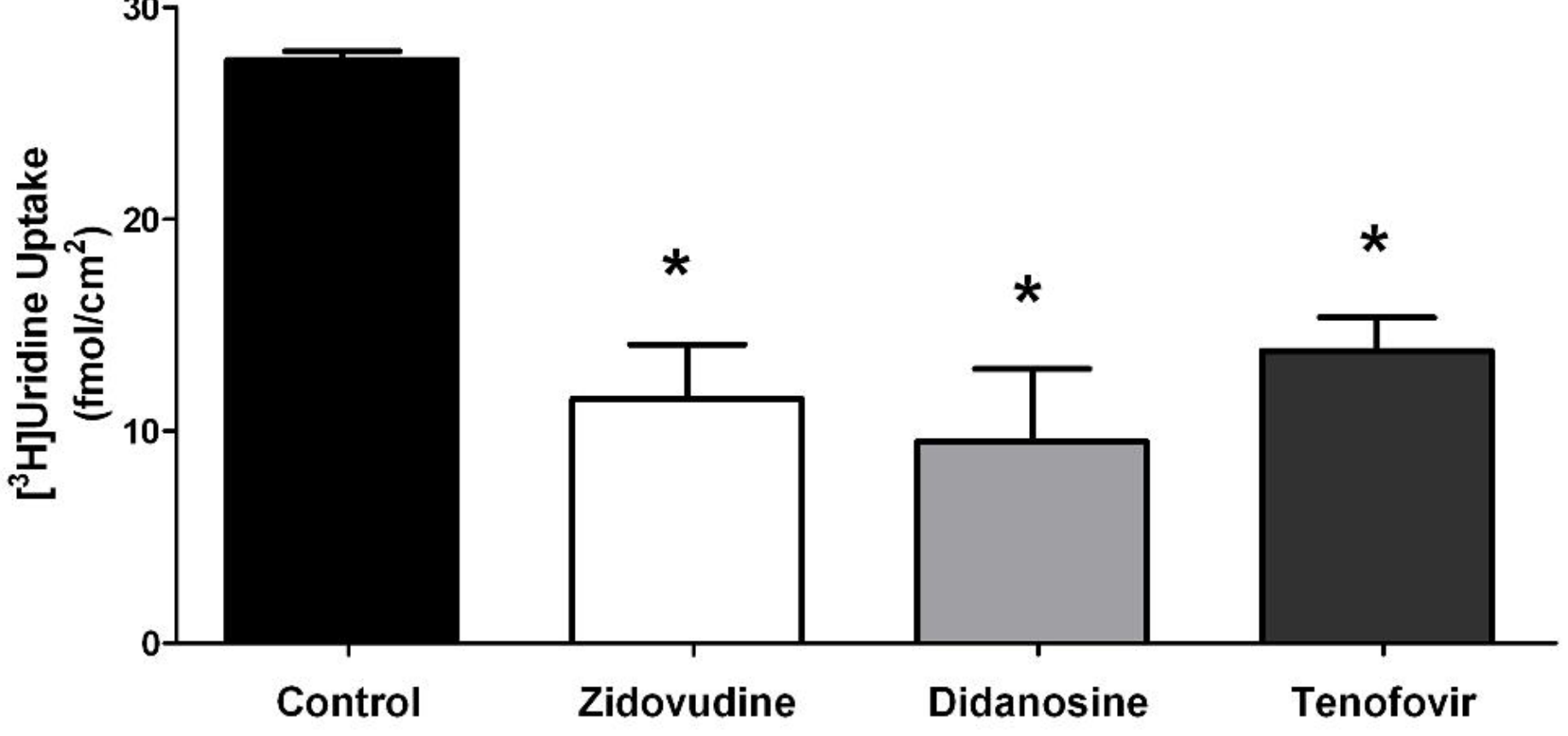
30
20
10
0
[3H]Uridine Uptake
(fmol/cm2)
*
*
*
Control
Zidovudine
Didanosine
Tenofovir

Figure 10

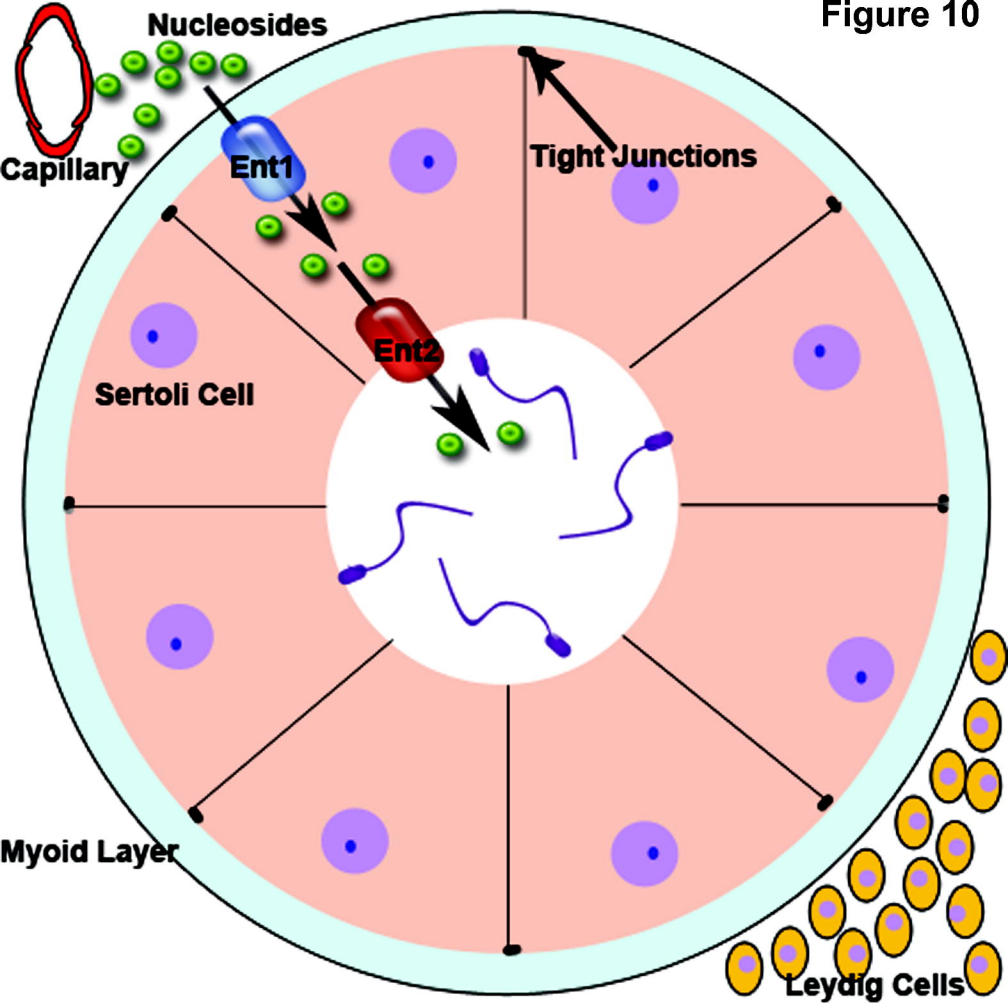
Nucleosides
Capillary
Ent1
Tight Junctions
Ent2
Sertoli Cell
Myoid Layer
Leydig Cells